

# First results from the Isaac Newton Telescope Wide Angle Survey: The $z > 5$ quasar survey

Sharp R.G., McMahon R.G., Irwin M.J., Hodgkin S.T.

*Institute of Astronomy, Madingley Road, Cambridge CB3 0HA, UK*

*Email: rgs, rgm, mike, sth@ast.cam.ac.uk*

Accepted ???. Received ???; in original form Latex version: 2001, Mar 05

## ABSTRACT

We report the first results of an observational program designed to determine the luminosity density of high redshift quasars ( $z > 5$  quasars) using deep multi-colour CCD data. We report the discovery and spectra of 3  $i < 21.5$  high redshift ( $z > 4.4$ ) quasars, including one with  $z > 5$ . At  $z = 5.17$ , this is the fourth highest redshift quasar currently published. Using these preliminary results we derive an estimate of the  $M_B < -25.0$  ( $M_{AB1450} < -24.5$ ) quasar space density in the redshift range  $4.8 < z < 5.8$  of  $3.6 \pm 2.5 \times 10^{-8} \text{ Mpc}^{-3}$ . When completed the survey will provide a firm constraint on the contribution to the ionizing UV background in the redshift range  $4.5 - 5.5$  from quasars by determining the faint end slope of the quasar luminosity function. The survey uses imaging data taken with the 2.5m Isaac Newton Telescope as part of the Public Isaac Newton Group Wide Field Survey (WFS). This initial sample of objects is taken from two fields of effective area  $\sim 12.5 \text{ deg}^2$  from the final  $\sim 100 \text{ deg}^2$ .

**Key words:** galaxies: active, quasars: general

## 1 INTRODUCTION

The identification and study of quasars at high redshift provides key diagnostic information on the early Universe. Over the last few years the relationship between high redshift quasars and local galaxies has been given an impetus from the realization that quiescent black holes may lie at the centre of all local bulges including the Milky Way (e.g. Magorrian et al., 1998). The formation and evolution of massive black holes is fast becoming a main stream topic in theories of galaxy formation and evolution (Haehnelt, Natarajan and Rees (1998); Kauffmann and Haehnelt (2000)).

High redshift quasars are also an important contributor to the UV radiation field in the early Universe. Specifically the lack of an optically thick, Gunn-Peterson trough in the spectra of high redshift objects (e.g. Songaila, Hu, Cowie, McMahon (1999)). implies that the Universe is highly ionized at  $z \sim 5.5$ . Estimates by Madau (1999) indicate that if the ionization is due to starlight the inferred star formation rate at  $z = 5$  must be comparable to or greater than the observed value at  $z = 3$ . The direct detection of galaxies at  $z \sim 3$  via the Lyman Break technique and the detection of measurable Lyman continuum photons that escape these galaxies (Steidel, Pettini and Adelberger (2001)) has raised a question over whether quasars or galaxies are the origin of the UV photons that re-ionized the Universe at  $z > 6$ . Recent theoretical work (Miralda-Escude, Haehnelt and Rees (1998); Madau, Haardt and Rees (1999)) indicates that a Gunn-Peterson

trough should be present by  $z \sim 6$ . A major uncertainty in all of this work is a measure of the ionizing background from quasars. The current uncertainty in the contribution of quasars to the UV background is predominantly caused by the unconstrained faint end of the luminosity function.

The recent discovery of several  $z > 5$  quasars by the Sloan Digital Sky Survey (SDSS Fan et al. (2001)) will constrain the bright end ( $i < 20.0$ ) of the high redshift luminosity function. We are undertaking a survey 1-2 magnitudes fainter than the SDSS program with the aim of constraining the space density and evolution of lower luminosity quasars where the majority of the ionizing flux arises. In this paper we present results from the first  $\sim 10 \text{ deg}^2$  of our survey. Unless stated otherwise we use conventional Vega magnitudes and  $H_0 = 50 \text{ km s}^{-1} \text{ Mpc}^{-1}$ ,  $q_0 = 0.5$ .

## 2 SURVEY IMAGING DATA

We are using data from the Isaac Newton Telescope (INT) Wide Angle Survey (WAS) (McMahon et al. (2000); <http://www.ast.cam.ac.uk/~wfcSUR/>). The survey is carried out with the prime focus Wide Field camera (WFC; Ives, Tulloch and Churchill (1996)) at the 2.5m INT. The WFC consists of a close packed mosaic of 4 thinned EEV42  $2k \times 4k$  CCDs. with a pixel size of  $13.5 \mu\text{m}$  corresponding to  $0.33''/\text{pixel}$  and effective field of view of  $0.25 \text{ deg}^2$ . The survey consists of single 600secs exposures in 5 wavebands

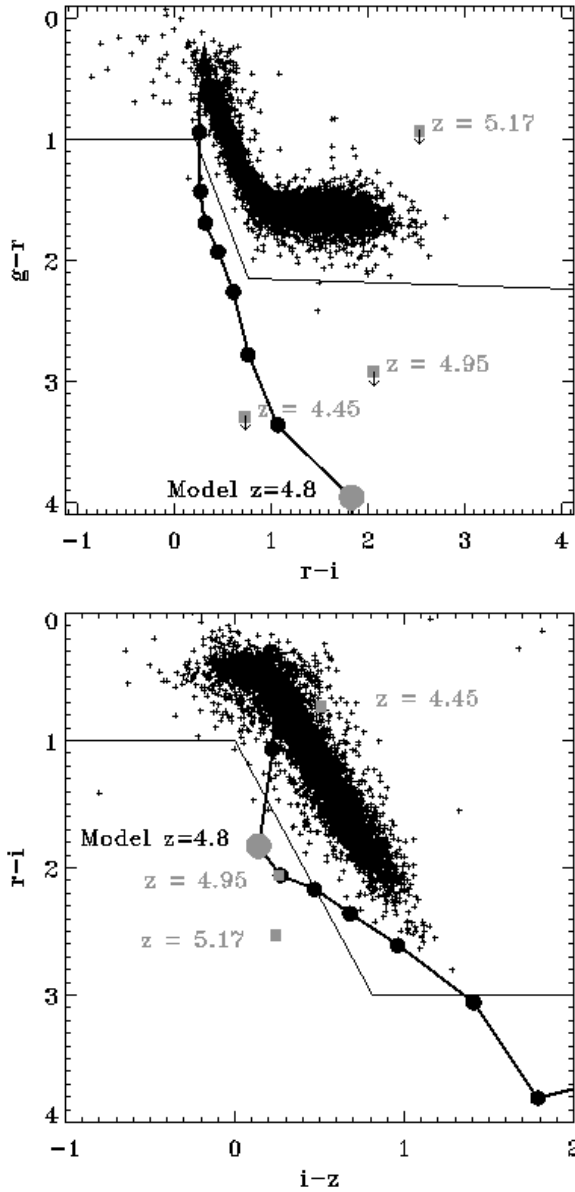


**Figure 1.** The *gri* and *riz* two-colour diagrams. Data from 8 pointings ( $\sim 2\text{deg}^2$ ) of the INT WFS is shown. All objects are classified as stellar and have  $i < 21.5$ . The newly discovered quasars (overplotted as squares) sit apart from the stellar locus. A model colour evolution track for quasars is overlaid. Filled circles indicate a 0.2 step in redshift from the larger circle at a redshift of 4.8 in this model.

(*ugriz*) over an area  $\sim 100\text{deg}^2$  to a nominal  $5\sigma$  limiting magnitude (Vega) of 23, 25, 24, 23 and 22 respectively.

The CCD mosaic data from all survey runs is pipeline processed in Cambridge (Irwin and Lewis (2000)) to produce photometrically and astrometrically calibrated images ( $\text{rms}(\text{internal})=0.1''$ ), and morphologically classified merged multicolour catalogues. A preliminary photometric calibration has been applied to the data to the  $\pm 0.1$  magnitude level. For the current work we have only used data with seeing of  $< 1.67$  arcsec (FWHM of 5 pixels) and stellar ellipticity (due to trailing) of better than  $< 0.2$  since this defines a practical upper limit for reliable image morphological classifica-

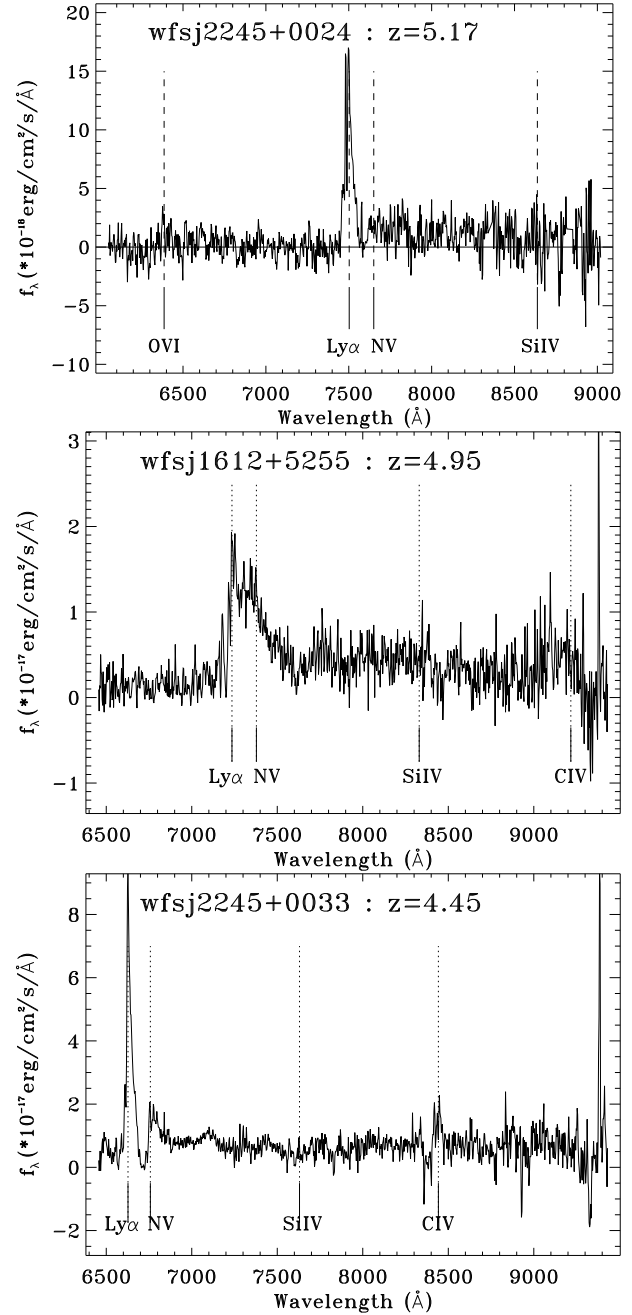


**Figure 2.** Quasars are readily identified, even at low signal-to-noise, by the characteristic continuum break across the prominent Lyman- $\alpha$  emission line. The identification of low level emission lines due to O VI, Si IV and C IV at the correct wavelengths relative to Lyman- $\alpha$  support the redshift estimation for these objects.

tion. The current quasar candidate sample has a magnitude limit of  $i$  or  $z < \approx 21$ , the practical limit for acceptable signal-to-noise spectra with a 4m class telescope in 1800 seconds of observation.

At the time of the spectroscopic follow-up observations in June 2000, object catalogues for data taken between August 1998 and October 1999 were available. This data is taken from two regions of the survey. The first region covers the ISO ELAIS N1 field at J1610+5430 (Oliver et al. (2000)),

**Table 1.** Photometry derived from the INT WFS.

Object	$z$	RA (J2000) Dec		$u$	Vega system magnitudes				$z$	$M_B$	$M_{AB(1450)}$
					$g$	$r$	$i$				
wfsj224524.2+002414	5.17	22 45 24.28	+00 24 14.6	>23.01	>24.89	23.96	21.43	21.19	-24.9	-24.3	
wfsj161253.1+525543	4.95	16 12 53.11	+52 55 43.5	>23.00	>25.12	22.21	20.15	19.89	-26.1	-25.6	
wfsj224531.0+003358	4.45	22 45 31.00	+00 33 58.6	>23.09	>24.89	21.60	20.87	20.36	-25.5	-25.0	

the second region is in the vicinity of at J2240+0000. A total area of  $12.5 \text{ deg}^2$  has been used.

### 3 COLOUR SELECTION OF CANDIDATES

Figure 1 shows colour-colour plots for INT WFS data in the *griz* bands with the predicted quasar tracks as a function of redshift overplotted. These colour tracks were computed assuming an underlying quasar spectrum based on a power law with spectral index ( $S_\nu \propto \nu^{-0.5}$ ) and with an emission line spectrum based on the composite spectrum of Vanden Berk et al. (2001). The absorption model for the intervening Lyman- $\alpha$  forest is taken from Madau (1995). The stellar main sequence is clearly visible as the heavily populated strip in the centre of the plots.

Candidate high redshift objects are selected from the multi colour data by selecting all objects that obey a set of colour criteria. To establish these criteria the stellar locus in the colour-colour diagrams has been approximated using piecewise linear fits in the colour space. These fits are then used to establish the boundaries indicated in Figure 1.

Once selected by one of these colour criteria all 5 *ugriz* images of an object are then visually examined to check the validity of the photometry. This step is required to identify spurious sources such as objects in the diffraction spikes of bright stars or satellites and asteroids that have moved significantly between observations. Candidate  $z \geq 5$  quasars are selected using the *riz* diagram whereas  $4 \leq z \leq 5$  candidates are selected from the *gri* colour diagram. At the current time the followup of the lower redshift sample is incomplete due to limited spectroscopic time.

### 4 SPECTROSCOPIC OBSERVATIONS

Spectroscopic observations were obtained in two nights (29th and 30th of June 2000) using the red arm of the ISIS dual beam spectrograph on the 4.2 meter William Herschel Telescope on La Palma. The R158R grating was used with the TeK4 CCD giving a spectral resolution of  $2.90 \text{ \AA}$  per pixel and wavelength coverage of  $2970 \text{ \AA}$ . Initially a central wavelength of  $7900 \text{ \AA}$  was selected but during observations it became apparent that a useful spectrum could not be taken of faint objects longward of  $9000 \text{ \AA}$  due to strong night sky line emission and so a central wavelength of  $7500 \text{ \AA}$  was subsequently used.

The slit width was matched to the seeing which varied over the course of the observing run in the range  $0.8''$ – $1.2''$ . During the periods of poorer seeing ( $\geq 1''$ ) brighter candidate objects were observed. These generally proved to be low mass late M and early L stars as expected. Conditions were photometric throughout the run and observations

of the spectrophotometric standards HZ 44, Ross 640 and LDS 749B (ING identifiers sp1321+363, sp1626+368 and sp2129+000) were used to flux calibrate the data. Wavelength calibration was carried out using a mixture of arc spectra and night sky lines.

Each observation was taken as a series of 900 second exposures and coadded to improve cosmic ray rejection. Total exposure times range from 900–2700 seconds. Several candidate objects could be identified as late M and early L dwarf stars after only a single 900 second exposure. Observation of these objects was truncated reducing the time spent observing non-quasar candidates.

### 5 CONFIRMED HIGH REDSHIFT QUASARS

The identification spectra of the confirmed high redshift ( $z > 4.4$ ) quasars are shown in Figure 2 and the emission line properties are presented in Table 2. Absolute B(Vega) band magnitudes and AB magnitudes at a rest-frame wavelength of  $1450 \text{ \AA}$  have been determined from the *z* band magnitudes assuming a power law spectral index of  $-0.5$ . We use the *z* band since it is unaffected by the Lyman- $\alpha$  forest or any strong emission lines.

Redshift determination for high redshift objects is complicated since in many spectra the only strong line visible is Lyman- $\alpha$  ( $1215.7 \text{ \AA}$ ). This is often blended on the red side with N V emission ( $1240.1 \text{ \AA}$ ) in quasar spectra and has an asymmetric profile due to absorption of the blue wing of the line by the Lyman- $\alpha$  forest. The onset of this absorption of the blue wing of the line is quite abrupt and we take this as our redshift estimate for the quasars.

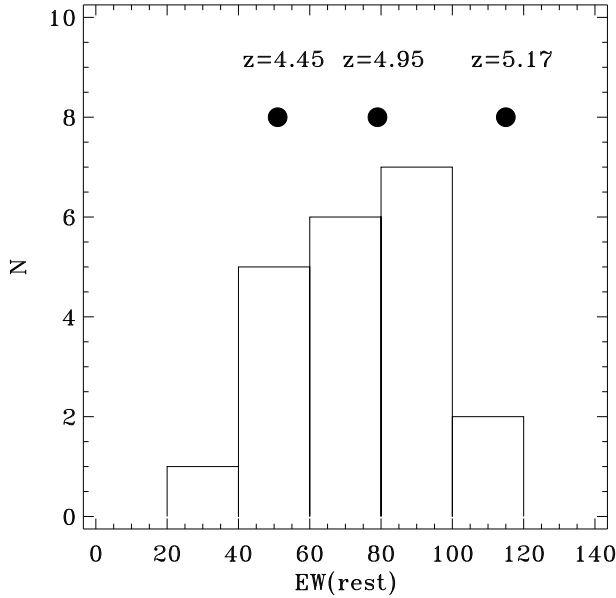
**wfsj224524.2+002414** At  $z=5.17$ , this is currently the fourth highest redshift quasar known. This faint object is identified by the strong Lyman- $\alpha$  line at  $7498 \text{ \AA}$  and the break in the continuum across the line due to Lyman- $\alpha$  forest absorption. Lyman- $\alpha$  shows a highly irregular profile with strong absorption features within the line. A strong absorption feature is also at the expected wavelength of N V emission redward of Lyman- $\alpha$ .

**wfsj161253.1+525543** This object shows a broad emission feature interpreted as a blend of Lyman- $\alpha$  and N V. The wavelength of any associated C IV emission line is in a region of the spectrum heavily effected by emission from the night sky making detection of an emission feature difficult. At  $z=4.95$  this quasar is the seventh highest redshift quasar known.

**wfsj224531.0+003358** Strong Lyman- $\alpha$  emission dominates the spectra of this object. Two clear absorption features, characteristic of the class of Broad Absorption line (BAL) quasars, are seen associated with N V and C IV emission lines.

**Table 2.** Emission line properties

Object	z	Lyman- $\alpha$		EW <sub>obs</sub>	EW <sub>rest</sub>	Cent.(z)	CIV	
		Peak (z)	Cent.(z)				EW <sub>obs</sub>	EW <sub>rest</sub>
wfsj2245+0024	5.17	7498Å (5.17)	7450Å (5.16)	594Å	115Å			
wfsj1612+5255	4.95	7237Å (4.95)	7318Å (5.00)	470Å	79Å	9112Å (4.88)	308Å	52Å
wfsj2245+0033	4.45	6628Å (4.45)	6634Å (4.46)	276Å	51Å	8400Å (4.42)		

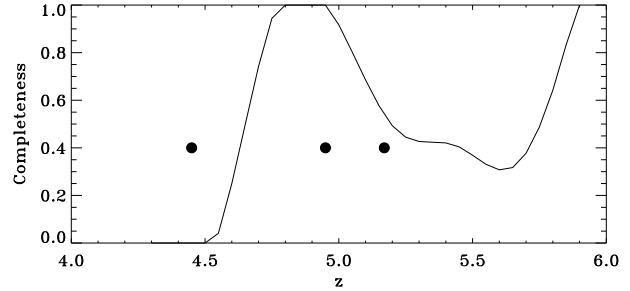
**Figure 3.** The histogram of Lyman- $\alpha$  equivalent width for SDSS quasars with redshift  $z > 4.4$  is shown with the measurements from the three  $z > 4.4$  INT WFS quasars over plotted for comparison.

The FIRST and NVSS radio surveys (Becker et al. (1995); Condon et al. (1998)) cover our survey regions and no radio emission with  $S_{20\text{cm}} > 1\text{mJy}(5\sigma)$  is detected for these quasars. There is also no evidence for X-ray emission from ROSAT All Sky Survey or PSPC pointed phase observations.

Figure 3 shows the equivalent width distribution of Lyman- $\alpha$  for the SDSS  $z > 4.4$  quasars compared with our new quasars. Despite the strength of the line in our  $z=5.17$  quasar it is comparable with the strongest lined objects in the SDSS sample.

## 6 DISCUSSION AND CONCLUSIONS

The majority of the  $\sim 250$   $z > 4$  quasars that are currently known (see <http://www.ast.cam.ac.uk/~quasars>) have been discovered using photographic plates but despite the relative ease with which  $z > 4$  quasars can be discovered (e.g. Storrie-Lombardi et al. (2000) and refs therein) for almost a decade the highest redshift object known was the optically selected quasar PC1247+3406 with  $z=4.89$  (Schneider et al. 1991). The addition of the  $z$  band to multi-colour surveys has changed this. The first quasars with  $z > 4.9$  was discovered by Fan et al. (1999) using SDSS data in the  $griz$  bands. In this paper we report two new quasars at  $z > 4.9$  bringing

**Figure 4.** An estimate of the survey completeness is derived based on the model quasar spectrum described in the text. The fractional completeness is shown as a function of redshift. The confirmed quasars are marked as black circles. At the current limiting magnitude the survey is not sensitive to photometric errors and so there is little change in completeness with magnitude.

the total sample of published quasars with redshift  $z > 4.9$  to nine, of which 6 have  $z \geq 5$  (see Table 3).

We use our sample to make the first estimate of the space density of low luminosity quasars at  $z \sim 5$ . Figure 4 shows the completeness of our survey with redshift. At the current magnitude limit for the spectroscopic sample the survey is not sensitive to photometric errors and so there is no magnitude effect on completeness. This has been computed using the approach described in Fan et al. (2001) where we use the Madau (1995) IGM model and an intrinsic unabsorbed quasar spectrum with a power law continuum spectrum with a gaussian distribution of spectral indices (mean =  $-0.5$ ; dispersion  $(\sigma) = 0.3$ ) and an contribution from emission lines. The relative emission lines strengths are taken from the SDSS composite quasar spectrum (Vanden Berk et al. (2001)) normalised to a Lyman- $\alpha$  line strength distribution (Rest frame Equivalent Width: Gaussian with mean 92.91 and sigma 24.0) from Wilkes et al. (1986). Using this completeness we calculate the effective volume assuming  $H_0 = 50 \text{ km s}^{-1} \text{ Mpc}^{-1}$ ,  $q_0 = 0.5$ .

The INT WFS is ongoing and to date  $\sim 10\%$  of the final survey imaging data has been investigated for candidate quasars. The final survey is expected to contain 10–20 high redshift ( $z > 5$ ) low luminosity quasars ( $i < 21.5$  and should therefore constrain the luminosity density to  $\sim 20\%$ . This statistically significant sample of low luminosity quasars will allow the determination of the faint end slope of the quasar luminosity function and the break point in the distribution (analogue to  $L^*$  for galaxies). This break point is required to allow estimation of the contribution of quasars to the ionizing UV background at high redshift. Our results, when combined with shallower surveys such as the SDSS, will allow detailed studies of the AGN phenomenon at high redshift over a range of UV luminosities. Our knowledge of the rela-

**Table 3.** Known High redshift ( $z > 4.9$ ) quasars

Name	$z$	Mag			$M_B$	Ref
		$r$	$i$	$z$		
wfsj2245.6+0024	5.17	23.96	21.43	21.19	-24.9	1
wfsj1612.7+5255	4.95	22.21	20.15	19.89	-26.1	1
SDSS1044-0125	5.80	>22.83	21.40	18.67	-27.5	2
RD J0301+0020	5.50	26.2	23.38	22.84	-23.4	3
SDSSp J1208+0010	5.27	22.66	20.37	20.17	-26.0	4
SDSSp J1204-0021	5.03	20.72	18.89	18.56	-27.5	5
SDSSp J0338+0021	5.00	21.61	19.54	19.19	-26.8	6
SDSSp J1605-0112	4.92	22.42	19.36	19.37	-26.6	5
SDSSp J0211-0009	4.90	21.97	19.51	19.26	-26.7	6

Refs: 1. This work; 2. Fan et al. (2000b); 3. Stern et al. (2000); 4. Zheng et al. (2000); 5. Fan et al. (2000a); 6. Fan et al. (1999);

tionship between accretion and the formation of black holes and galaxies will then not rely purely on the properties of the rare extreme luminosity quasars.

## ACKNOWLEDGMENTS

RGS acknowledges the receipt of a PPARC studentship. RGM thanks the Royal Society for support. This paper uses data that was made publically available through the Isaac Newton Groups' Wide Field Camera Survey Programme. The Isaac Newton Telescope is operated on the island of La Palma by the Isaac Newton Group in the Spanish Observatorio del Roque de los Muchachos of the Instituto de Astrofísica de Canarias.

## REFERENCES

- Becker R.H., White R.L. and Helfand D.J. 1995 ApJ 450 559  
 Condon J.J. et al. 1998 AJ 115 1693  
 Fan X. et al. 1999 AJ 118 1F  
 Fan X., Strauss M.A., Schneider D.P., Gunn J.E., Lupton R.H., Anderson S.F., 2000 AJ 119 1  
 Fan X. et al. 2000 AJ 120 1167  
 Fan X., Strauss M.A., Newman J.A., et al. 2001 AJ 121  
 Fan X. et al. 2001 AJ 121 54  
 Francis P.J. et al. , 1991, ApJ, 373, 465  
 Gunn J.E. Peterson B.A. 1965 ApJ 142 1633  
 Haehnelt, Natarajan & Rees 1998 MNRAS 300 817  
 Irwin M.J. , Lewis J.R. 2000, New Astronomy Reviews (in press).  
 Ives D.J., Tulloch S., Churchill J. 1996 SPIE 2654 266  
 Kauffmann G., Haehnelt M.G 2000 MNRAS 311 576  
 McMahon R.G. et al. 2000 arXiv:astro-ph/0001285  
 Madau P. 1995 ApJ, 441, 18  
 Madau P., Haardt F., Rees M. 1999 ApJ 514 648  
 Magorrian et al. 1998 AJ, 115 2285  
 Miralda-Escude, Haehnelt M., Rees M., arXiv:astro-ph/9812306  
 Oliver S. et al. arXiv:astro-ph/0003263  
 Schneider D.P., Schmidt, M., Gunn J.E. 1991 AJ, 102, 837  
 Schmidt M. Schneider D.P. Gunn J.E. 1995 AJ 110 68  
 Songaila A. Hu E. Cowie L. McMahon R.G. 1999 ApJ, 525, 5  
 Steidel C.C., Pettini M., Adelberger K.L. 2001 ApJ 546 665  
 Stern D. et al. 2000 ApJ 533 75  
 Storrie-Lombardi L.J., Irwin M.J., McMahon R.G., Hook I.M. arXiv:astro-ph/0012446

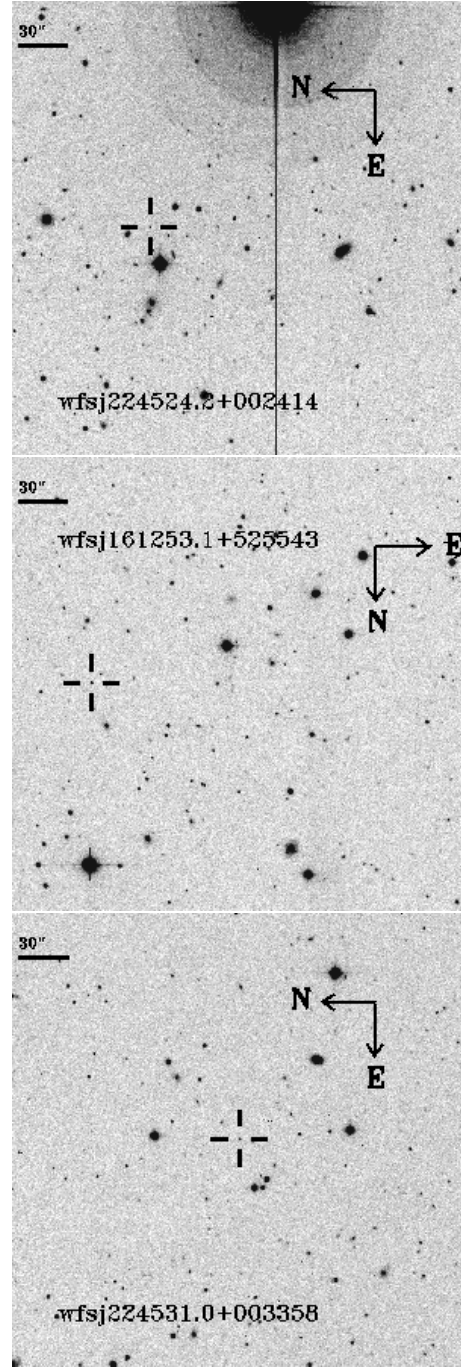


**Figure 5.** Finding charts are taken from  $i$  band images. The charts are 4.4 arcminutes (800 pixels) square with the quasar marked by the cross hair.

- Vanden Berk D.E. and SDSS Collaboration 2001 arXiv:astro-ph/0105231  
 Warren S., Hewett P., Osmer P. 1994 ApJ 427 412  
 Wilkes B.J. 1986 MNRAS 218 331  
 Zheng W. et al. 2000 AJ 120 1607